

# Hubble Space Telescope ultraviolet spectroscopy of blazars: emission lines properties and black hole masses

E. Pian<sup>1\*</sup>, R. Falomo<sup>2</sup>, A. Treves<sup>3</sup>

<sup>1</sup>INAF, Astronomical Observatory of Trieste, Via G.B. Tiepolo 11, I-34131 Trieste, Italy

<sup>2</sup>INAF, Astronomical Observatory of Padova, via dell'Osservatorio 5, I-35122 Padova, Italy

<sup>3</sup>Department of Physics and Mathematics, University of Insubria, Via Valleggio 11, I-22100 Como, Italy

Accepted ... Received 2005 January 20; in original form 2005 January 1

## ABSTRACT

The ultraviolet (UV) spectra of 16 blazars ( $< z > \simeq 1$ ) from the archives of the Hubble Space Telescope Faint Object Spectrograph have been analyzed in order to study in a systematic way the properties of their broad UV emission lines. We find that the luminosities of the most prominent and intense lines, Ly $\alpha$  and C IV  $\lambda$ 1549, are similar to those of normal radio-loud quasars at comparable redshifts. However, the equivalent widths of blazar lines are significantly smaller than those of radio-loud quasars. Therefore, while the intrinsic broad line region luminosity of blazars appears to be indistinguishable from that of radio-loud quasars, their continuum must be comparatively higher, most probably due to relativistic beaming. We have combined the UV luminosities of the de-beamed continuum with the emitting gas velocity to derive estimates of the masses of the central supermassive black holes. The size of the broad line region was computed in two ways: 1) via an empirical relationship between UV continuum luminosity and broad line region size, and 2) through the external photon density required by blazar models to reproduce the inverse Compton components observed at gamma-rays. The second method yields significantly different results from the first method, suggesting that it provides only a very rough estimate or a lower limit on the size of the broad line region. We find that the average mass of the central black holes in blazars is  $\sim 2.8 \times 10^8 M_{\odot}$ , with a large dispersion, comparable to those computed for other radio-loud active galactic nuclei.

**Key words:** galaxies: active — BL Lacertae objects — ultraviolet: galaxies — Gamma rays: observations

## 1 INTRODUCTION

Highly Polarized Quasars (HPQ, also referred to as Flat Spectrum Radio Quasars) and, occasionally, BL Lacertae objects, collectively known as blazars, exhibit broad emission lines superimposed on their optical and ultraviolet (UV) continua (Netzer et al. 1994; Scarpa, Falomo, & Pian 1995; Vermeulen et al. 1995; Corbett et al. 1996; Scarpa & Falomo 1997; Koratkar et al. 1998; Pian et al. 2002; D'Elia, Padovani, & Landt 2003). Emission lines play an important role in the energetics of blazars: some models of multi-wavelength blazar emission (Dermer & Schlickeiser 1993; Sikora et al. 1994; Ghisellini & Madau 1996) predict that the broad line region (BLR) photons are Compton upscattered to X- and gamma-ray energies by the relativistic particles composing the jet plasma, and form luminous high energy spectral components, which often dominate the overall blazar output (Mattox et al. 1997; Bloom et al. 1997; Wehrle et al. 1998; Hartman et al. 2001; Ballo et al. 2002; Pian et al. 2002). The role of broad line emission in shaping the

spectrum of different classes of blazars is however not fully assessed (Fossati et al. 1998; Ghisellini et al. 1998; Padovani et al. 2003).

More in general, the characteristics of the BLR of blazars may help in investigating the interplay between the accretion disk and the relativistic jet, which is more prominent in blazars than in normal QSO and Seyferts (Celotti et al. 1997; Maraschi & Tavecchio 2003; D'Elia et al. 2003; Wang, Luo, & Ho 2004). AGN broad emission lines may be used also to estimate the masses of the compact objects residing in the nuclear centers, most likely supermassive black holes (BH), by exploiting their dynamical effect on the line-emitting gas clouds. The application of the virial theorem requires that the size of the BLR is determined either with direct methods (reverberation mapping technique, Peterson & Wandel 2000; Kaspi et al. 2000; Peterson et al. 2004), or with indirect arguments (Kaspi et al. 2000; Vestergaard 2002). In the latter case the uncertainties are obviously larger, and the methods must be tested carefully. Since this has important consequences on the evolution and demographics of AGNs, it is crucial to accomplish these measurements both for low and high redshift sources. This approach has been adopted in the estimate of BH masses of large

\* E-mail: pian@ts.astro.it (EP); falomo@pd.astro.it (RF); Aldo.Treves@uninsubria.it (AT)

samples of quasars based on optical emission lines (Woo & Urry 2002; McLure & Dunlop 2004). The advantage of using UV, rather than optical emission lines is that the former correspond to a higher ionization state and are therefore presumably more representative of the dynamics close to the central massive object.

In this paper we present the analysis of the broad and intense UV emission lines of 16 blazars observed by the Hubble Space Telescope (HST) and the Faint Object Spectrograph (FOS). Previous studies of AGN UV spectra have been carried out by Bechtold et al. (2002), who focussed on the absorption systems, by Kuraszkiwicz et al. (2002) and Kuraszkiwicz et al. (2004), who present a complete HST FOS atlas of emission line parameters of AGNs, and by Evans and Koratkar (2004), who recalibrated the pre-COSTAR AGN spectra. We concentrate here on the UV spectra of blazars. Based on the radiative and kinematic properties of the broad emission line region (BLR), we measure the luminosities of their BLRs and derive estimates of the BLR sizes and of the central BH masses.

We adopt the “concordant cosmology”,  $\Omega_m = 0.3$ ,  $\Omega_\Lambda = 0.7$ , and assume  $H_0 = 72 \text{ km s}^{-1} \text{ Mpc}^{-1}$  (Spergel et al. 2003). Luminosities reported by other authors and used in this paper have been transformed into this cosmology.

## 2 SAMPLE SELECTION AND DATA ANALYSIS

We have retrieved from the HST archive<sup>1</sup> all pre- and post-COSTAR FOS grating spectra of sources previously classified as blazars (Wall & Peacock 1985; Impey & Tapia 1988; Impey & Tapia 1990; Impey et al. 1991; Stickel et al. 1991; Stocke et al. 1991; Padovani & Urry 1992; Wills et al. 1992; Perlman et al. 1996). We also included in our final list PKS 1229-021, which, despite having low polarization (Wills et al. 1992), is considered a blazar because of significant emission at MeV-GeV frequencies (Hartman et al. 1999), and 3C 273, which has intermediate properties between those of blazars (strong radio emission, superluminal motion, gamma-ray emission, jet emission dominance at hard X-ray energies, e.g., Haardt et al. 1998; Grandi & Palumbo 2004), and those of Seyfert galaxies (broad emission lines, big blue bump). We selected spectra taken with high-resolution gratings in the UV region (G130H, G190H, G270H, G400H).

This search yielded 24 objects with measurable spectra. Spectra taken with the same grating within one day were averaged to increase the signal-to-noise ratio. For this work we have considered only the 16 sources with significant (larger than  $3\sigma$ ) emission line detections. These are reported in Table 1.

For 6 sources there are also low-resolution grating (G160L) observations in the archive, obtained nearly simultaneously to the high-resolution spectra (i.e., within one day). Since the line parameters and spectral indices derived from the former are not significantly different from those measured in the high-resolution spectra, we have neglected these spectra.

Although the considered objects do not represent a complete sample, they form a sizeable dataset to investigate the UV line properties of blazars.

After applying a correction for the Galactic absorption using the maps of Schlegel, Finkbeiner and Davis (1998) and the extinction curve of Cardelli, Clayton and Mathis (1989), we measured

the equivalent widths (EWs), the intensities and the full width at half maximum (FWHM) values of the emission lines fitting a linear local continuum on each side of the line (see Table 2). The EW uncertainties were estimated by assuming  $2\sigma$  variations of the local continuum.

For each object we have combined the spectra taken quasi-simultaneously (within 1 day) with different gratings, excluded the regions affected by emission or absorption features, binned the signal in 20-50 Å wavelength intervals and fitted the continuum with a power-law. To account for calibration uncertainties of the data, we added a 5% systematic error to the statistical errors. The derived power-law spectral indices and flux normalizations are given in Table 1.

A similar analysis of the continuum and line properties of these objects has been presented in Kuraszkiwicz et al. (2002) and Kuraszkiwicz et al. (2004).

## 3 RESULTS

The redshifts of our objects (see Table 1) range between  $z = 0.158$  and  $z = 1.404$ , with an average value of  $\langle z \rangle = 0.84 \pm 0.31$ . Thus, the lines typically detected in our FOS spectra are Ly $\beta$ , Ly $\alpha$ , C IV  $\lambda 1549$ , C III]  $\lambda 1909$ , Si IV  $\lambda 1400$  and in some cases Mg II  $\lambda 2798$ . We report in Table 1 the spectral indices and normalizations of the UV continua and in Table 2 the EW and the FWHM values of the emission lines.

In 3 cases (3C 273, 3C 345, and 3C 454.3) observations at more than one epoch are available. Variations of line and continuum emission are observed, with maximum amplitudes of factors of  $\sim 2$  and 7, respectively. However the observations are too limited and sparse to allow a meaningful assessment of correlated line and continuum variability.

In section 3.1 we describe the average properties of the emission lines of blazars in the UV spectral region; in section 3.2 we use the line and continuum properties of the UV spectra to estimate the masses of the central BHs.

### 3.1 Emission line properties

In order to produce a representative high signal-to-noise ratio UV spectrum of blazars, we have combined all the UV spectra in our dataset. Each spectrum was first reduced to rest-frame and then normalized to its average continuum flux. The resulting composite blazar spectrum, normalized to unity at the reference wavelength of 1500 Å, is shown in Fig. 1. The EW, relative intensities, and FWHM of the emission lines of the composite spectrum are given in Table 3.

The composite spectrum of blazars is similar to that of normal QSO. The line ratios of blazars and normal AGNs are also not significantly different. This is illustrated in Fig. 2, where we report the luminosities of the Ly $\alpha$  and C IV  $\lambda 1549$  lines of blazars, compared with those of a list of radio-loud quasars (RLQ) observed by HST FOS (Wills et al. 1995). Note that in this list of RLQ there are 8 objects in common with our sample of blazars; therefore, for the purpose of the comparison, these 8 sources have been considered as blazars and have been excluded from the RLQ list. We also compare with the RLQ 3C 390 (1845+79,  $z = 0.056$ ), which has hybrid properties, i.e., it has substantial polarization (1.3%, Impey et al. 1991), but is lobe-dominated at radio wavelengths (Ghisellini et al. 1993). Figure 2 shows that the intensity ratio of Ly $\alpha$  vs the

<sup>1</sup> using MAST, the Multi-mission Archive at STScI, see <http://archive.stsci.edu>.



**Table 3.** Composite ultraviolet blazar spectrum.

Line	EW <sup>a</sup>	FWHM <sup>a</sup>	Rel. Intensity <sup>b</sup>	Ratio <sup>c</sup>	Ratio (LBQS) <sup>d</sup>	Ratio (RLQa) <sup>e</sup>	Ratio (RLQb) <sup>f</sup>
Ly $\beta$	6.5 $\pm$ 0.5	10	8.9 $\pm$ 0.5	10.6	9.3	19	19.1
Ly $\alpha$	71 $\pm$ 3	22	84 $\pm$ 3	100	100	100	100
SiIV	5.2 $\pm$ 0.7	21	5.6 $\pm$ 0.7	6.6	19	6.8	8.6
C IV	45 $\pm$ 2	20	45 $\pm$ 1	53	63	66	52
C III]	7 $\pm$ 1	23	6.6 $\pm$ 0.7	7.8	29	11	13.2
Mg II	19 $\pm$ 2	30	16 $\pm$ 1	19	34	24	22.3

<sup>a</sup> At rest frame, in  $\text{\AA}$ . Uncertainties are about  $\sim 15\%$ .

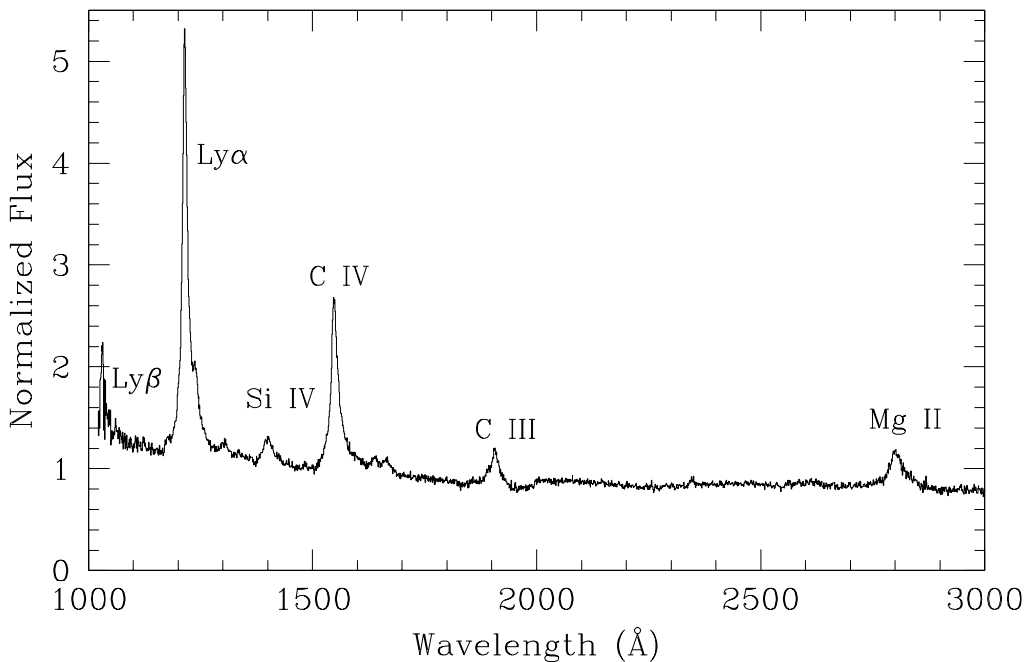
<sup>b</sup> Obtained from EW and continuum normalized to the flux at 1500  $\text{\AA}$  (rest frame).

<sup>c</sup> Average percentage intensity ratio with respect to Ly $\alpha$  as resulting from our measurements.

<sup>d</sup> Same as in Col. 5 for 718 objects in the Large Bright Quasar Survey (Francis et al. 1991).

<sup>e</sup> Same as in Col. 5 for for 60 radio loud quasars (Zheng et al. 1997).

<sup>f</sup> Same as in Col. 5 for 107 radio loud quasars (Telfer et al. 2002).

**Figure 1.** Composite UV spectrum of blazars obtained from the average of 16 spectra. The most prominent emission lines are labeled.

the Keplerian velocities of the line-emitting material in a virialized system (Wandel et al. 1999; McLure & Dunlop 2001), the BH mass  $M_{BH}$  is given by:

$$M_{BH} = G^{-1} v^2 R_{BLR} \quad (2)$$

where  $v$  is the velocity of the gas gravitationally bound to the central BH,  $R_{BLR}$  is the size of the BLR, and  $G$  is the gravitational constant. The velocity  $v$  can be obtained directly from the FWHM of the broad emission lines ( $v = f \times v_{FWHM}$ ), where  $f$  is a fac-

tor that depends on the geometry and kinematics of the BLR (e.g., McLure & Dunlop 2002; Vestergaard 2002).

### 3.2.1 Size of the BLR

The most reliable method to derive  $R_{BLR}$  is through the reverberation mapping technique (e.g. Peterson et al. 2004, and references therein). This uses the time lag of the emission line light curve with respect to the continuum light curve to determine the light crossing size of the BLR in AGNs. However, this method requires inten-

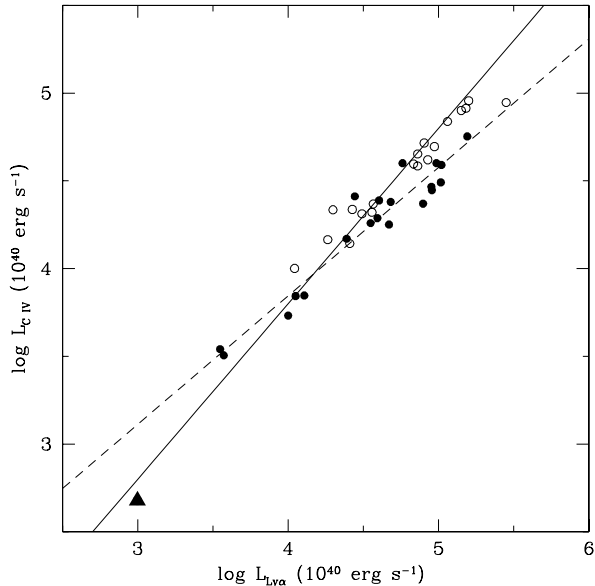


**Figure 2.** Luminosities of C IV  $\lambda 1549$  and Ly $\alpha$  emission lines for the blazars in our list (filled circles). Line measurements of a given source at multiple epochs have not been averaged. The Ly $\alpha$  and C IV  $\lambda 1549$  emission line intensities have been normalized to their respective average values. The solid line is the expected C IV  $\lambda 1549$  to Ly $\alpha$  intensity ratio ( $L(\text{C IV } \lambda 1549) = 0.63 \times L(\text{Ly}\alpha)$ , e.g. Francis et al. 1991). The dashed line is the least square regression line  $L(\text{C IV } \lambda 1549) = 8.3 \times L(\text{Ly}\alpha)^{0.73}$ . For comparison, the line luminosities of 19 RLQ (open circles) from Wills et al. (1995) and of 3C 390 (triangle) are also shown.

sive monitoring of the UV continuum and of the lines and can be used only for a limited number of objects (e.g., Korista et al. 1995; Onken et al. 2002), including one of our sources, 3C 273 Paltani & Türler 2005). An alternative way to estimate  $R_{\text{BLR}}$  is to use the empirical relationship found between  $R_{\text{BLR}}$  and the optical continuum luminosity (Kaspi et al. 2000).

We have derived this relationship in the UV for a sample of 15 PG quasars and 10 Seyfert 1 galaxies having BLR radii determined via reverberation mapping in the optical (Kaspi et al. 2000) and measured UV spectra (Vestergaard 2002). One of the PG quasars is 3C 273, which is also a member of our blazar sample. For this object, we corrected the continuum luminosity for the beaming effect (see Eq. 1). For one of the Seyferts, NGC 4151, the UV continuum of which varies with high amplitude, we re-measured the continuum luminosity at 1350 Å from the average IUE spectrum. These quantities are reported in Fig. 4. We fitted the BLR radii and the luminosities at 1350 Å (rest frame) with a power-law and obtained the following relationship:

$$R_{\text{BLR}} = (22.4 \pm 0.8) \left( \frac{\lambda L_{\lambda}(1350\text{\AA})}{10^{44} \text{erg s}^{-1}} \right)^{0.61 \pm 0.02} \text{lt - days} \quad (3)$$

If we exclude 3C 273 from the fit, the result is unchanged (the power-law index is  $0.60 \pm 0.02$  in this case). We note that the slope in Eq. 3 is consistent with that determined in the same wavelength range by Kaspi et al. (2005, index  $0.56 \pm 0.05$ ), it is slightly flatter than that found in the optical by Kaspi et al. (2000, index  $0.70 \pm 0.03$ ) and slightly steeper than that found by McLure and

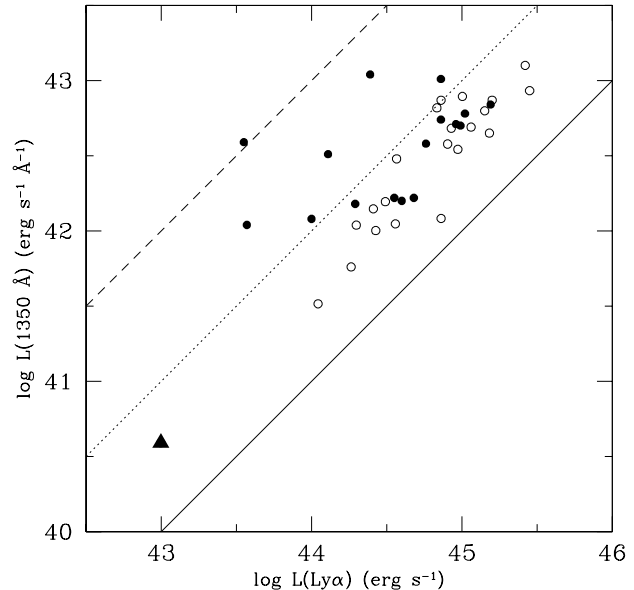


**Figure 3.** Ly $\alpha$  luminosity vs continuum luminosity at 1350 Å (rest frame) for blazars (filled circles) and RLQs (open circles). The triangle represents the low redshift RLQ 3C 390. The lines are the loci of the EW = 10 Å (dashed), 100 Å (dotted) and 1000 Å (solid).

Jarvis (2002, index  $0.50 \pm 0.02$ ) at 3000 Å, based on a very similar sample of PG quasars and Seyfert galaxies.

Since the relationship between the BLR radius and continuum luminosity is supposed to be valid in the case of a thermal continuum (see also discussion in Paltani and Türler 2005), we must correct the blazar UV continuum luminosities for the effect of relativistic beaming.

For the blazars with continuum luminosity exceeding the power-law dependence between the RLQ line and continuum luminosities (Eq. 1), we adopted the continuum luminosities computed with Eq. 1 at the corresponding line luminosity, and derived the BLR radii through Eq. 3. These are reported in Table 4. The correction of the continuum luminosity is relevant (i.e., larger than  $\sim 3$  times the scatter) for 4 objects (see Fig. 3). We note that our estimate of the BLR radius of 3C 273 is consistent with that reported by Paltani and Türler (2005).

An alternative, independent method for evaluating  $R_{\text{BLR}}$  consists in coupling the luminosity of the BLR with the information carried by the multiwavelength spectrum of the blazar. Since blazars, among all AGNs, are the only ones with a spectrum extending to gamma-rays, this method is specific for the blazar class of AGNs.

Ten of our blazars have multiwavelength energy distributions which have been fitted with synchrotron and inverse Compton radiation components (Ghisellini et al. 1998). The latter component dominates at the X- and gamma-ray energies and originates from the scattering of relativistic electrons off both synchrotron photons (internal to the jet) and external radiation fields. These include broad line photons, the density of which,  $U_{\text{ext}}$ , is thus estimated through the multiwavelength spectral fit.

Following the procedure adopted by Celotti, Padovani and

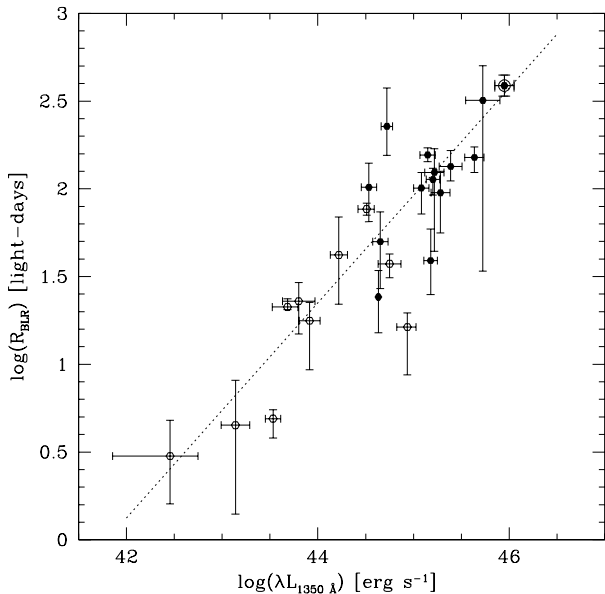


**Figure 4.** Size of the BLR as a function of the continuum power output at 1350 Å (rest frame) for the sample of PG quasars (filled circles) and Seyfert 1 galaxies (open circles) of Kaspi et al. (2000). The encircled point on the top right represents 3C 273. The luminosities have been taken from Vestergaard (2002). The line fitting the 2 quantities (Eq. 3) is also reported (dotted).

Ghisellini (1997), we reconstructed the total luminosity of the BLR for each of our sources by using the intensities of the observed UV emission lines and by assuming for the unobserved lines the line ratios of an average quasar spectrum (Francis et al. 1991). These derived BLR luminosities are reported in Table 4.

From the *fitted* densities of the external photons  $U_{ext}$  and from the *observed* BLR luminosities, the size of the BLR,  $R_{BLR}$ , can be derived according to:

$$R_{BLR} = \sqrt{\frac{L_{BLR}}{4\pi c U_{ext} \delta^2}} \quad (4)$$

where  $\delta$  is the relativistic Doppler factor required by the multiwavelength modeling. The BLR radii computed with Eq. 4 are reported in Table 4. We have identified this second method as “spectral energy distribution (SED) method”, in order to distinguish it from the one based on the empirical determination of  $R_{BLR}$  from the continuum luminosity. No clear correlation is found between the BLR radii determined with the two methods. One probable explanation of the discrepancy is that the radiation density of the BLR is generally smaller than the parameter  $U_{ext}$  obtained with multiwavelength fits. This parameter includes not only the BLR photons, but also additional contributions, such as photons coming directly from the accretion disk, or produced by the dusty torus, or by larger regions of the jet (Ghisellini priv. comm.). Thus, the SED method may underestimate the BLR sizes (and therefore the BH masses) in some cases. Moreover, the uncertainties associated with the SED fit parameters are large. Therefore, although we had proposed the “SED” method for BH mass determination in an individual source

(PKS 0537–441, Pian et al. 2002), it appears that this method cannot be generalized.

### 3.2.2 Mass estimates

In order to evaluate the BH masses of our objects we have used Eqs. 2 and 3, adopting a standard value of  $f = \sqrt{3}/2$  for the kinematic factor, corresponding to an isotropic distribution of the BLR clouds (Wandel 1999; Kaspi et al. 2000; Vestergaard 2002), that yields virial BH masses consistent with those derived from the  $M_{BH}$ - $L_{bulge}$  relationship (Labita, Falomo, & Treves, in prep.). After setting  $v_{FWHM}$  to suitable units we obtain the relation:

$$M_{BH} = 3.26 \times 10^6 \left( \frac{\lambda L_{\lambda}(1350\text{\AA})}{10^{44} \text{erg s}^{-1}} \right)^{0.61} \left( \frac{v_{FWHM}}{10^3 \text{ km s}^{-1}} \right)^2 M_{\odot} (5)$$

Vestergaard (2002) also derives a formula for the central BH mass, based on the continuum measurements at the rest frame wavelength of 1350 Å of a sample of 26 AGN with BLR radii determined by reverberation mapping. However, this relationship was calibrated against the BH masses determined from optical measurements, and not directly from the BLR size, as we do.

By using Eq. 5 with the beaming-corrected  $L(1350 \text{ \AA})$  luminosities and  $v_{FWHM}$  estimated from our spectra, we have computed the central BH masses. For consistency with Vestergaard (2002) we have used the FWHM of C IV  $\lambda 1549$ . These masses are reported in Column 5 of Table 4, and in Fig. 5, where they are compared with those computed with our Eq. 5 for a sample of PG quasars, for which Vestergaard (2002) reports UV luminosities and C IV  $\lambda 1549$  line FWHM values. The blazar BH masses are statistically consistent with those of quasars: the averages of the logarithmic distributions, in solar masses, are  $\langle \log M_{BH} \rangle = 8.31 \pm 0.10$  and  $\langle \log M_{BH} \rangle = 8.42 \pm 0.08$  for blazars and RLQ, respectively (the uncertainties represent the errors associated with the averages, i.e. the standard deviations divided by the square root of the number of objects).

For comparison, we have also computed the blazar BH masses using Vestergaard’s relationship (Eq. 8 of Vestergaard 2002), with our measured blazar luminosities and FWHM values of the C IV  $\lambda 1549$  line. These are systematically lower than the corresponding ones determined using Eq. 5, by a factor 1.4–2. We have also compared our estimated BH masses with those determined for the same blazars by other authors: a number of our objects are in common with the samples of Liang and Liu (2003), Woo and Urry (2002), and Wang et al. (2004). Their mass estimates have been reported in the last 3 columns of Table 4: our masses are generally smaller. This may be partially due to our correction of the continuum luminosity for the beaming effect. In particular, this must be the case for two of the four objects in our sample with the most strongly beamed continuum, 3C 279 and 0537–441.

We do not find a correlation of the BH mass with redshift for our blazar sample.

## 4 SUMMARY AND CONCLUSIONS

We have studied the properties of the UV emission lines of blazars, mostly from single epoch HST FOS spectra, and found that the average blazar UV spectrum is similar to that of RLQ. This is the sum of a thermal and non-thermal component. Our targets are mainly HPQ and Low-Frequency Peaked BL Lacs (Padovani & Giommi 1995; Fossati et al. 1998) where the emission of the non-thermal synchrotron component peaks at optical/IR frequencies. Therefore

**Table 4.** BLR Luminosities and Central Black Hole Masses.

Object	$L_{BLR}^a$	$R_{BLR}^b$	$R_{BLR,SED}^c$	$M_{BH}^d$	$M_{BH,LL}^e$	$M_{BH,WU}^f$	$M_{BH,W}^g$
BL0403-1316	22.6	145	...	2.4		12	
BL0420-0127	18.7	145	438	2.3	8	11	9
BL0537-4406	6.93	77	211	0.5	16		5
BL0637-7513	50.2	285	...	1.9		26	
BL0954+5537	5.38	66	312	0.5	8	1.2	
BL1144-3755	2.45	34	...	0.4			
BL1156+2931	13.7	115	158	4.3	8		
BL1226+0219	33.8	219	17	4.0	0.2		16
BL1229-0207	74.1	357	117	7.4	10		
BL1253-0531	2.42	36	104	0.8	4	2.7	3
BL1611+3420	34.1	196	92	6.2	40	37	
BL1641+3954	12.5	92	...	2.7		26	28
BL2223-0512	25.2	150	...	2.8			6
BL2230+1128	41.4	260	33	3.1	12.6		
BL2243-1222	47.8	271	...	2.1			
BL2251+1552	33.3	223	29	3.1	25	15	13

<sup>a</sup> Luminosity of the BLR, in units of  $10^{44}$  erg s<sup>-1</sup>.

<sup>b</sup> Size of the BLR computed via Eq. 3, in light days.

<sup>c</sup> Size of the BLR computed using the SED method, (Eq. 4), in light days.

<sup>d</sup> Mass of the central BH computed using Eq. 5, in units of  $10^8 M_{\odot}$ . The statistical uncertainties, dominated by the scatter of Eq. 3, are about a factor 2.

<sup>e</sup> Mass of the central BH from Liang & Liu (2003).

<sup>f</sup> Mass of the central BH from Woo & Urry (2002).

<sup>g</sup> Mass of the central BH from Wang et al. (2004).

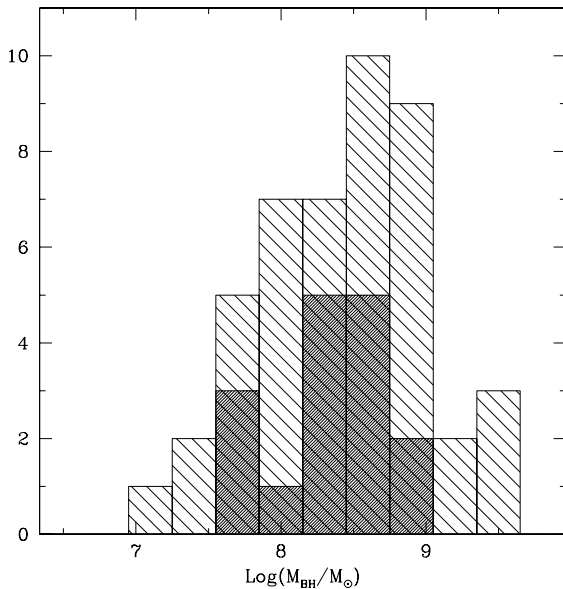


**Figure 5.** Histograms of central BH masses of AGNs. The simply hatched area represents the masses of PG quasars computed with Eq. 5 from the luminosities and C IV  $\lambda 1549$  emission line FWHM values reported by from Vestergaard (2002). The double-hatched area represents the BH masses of our blazar sample. Mass estimates obtained for a same source at different epochs have been averaged.

a large relative contribution from the thermal accretion disk is expected in the UV region (e.g., Bregman et al. 1986). This is clearly evident from the spectral energy distribution of 3C 273 (Ulrich et al. 1980; Courvoisier 1998) and may be significant in 3C 279 (Pian et al. 1999).

With the aim of estimating central BH masses of blazars, we have assumed Keplerian conditions in the BLR gas motion and have evaluated the BLR size using the results of a fit of UV luminosities and BLR radii of a sample of QSOs having BLR sizes determined via reverberation mapping in the optical. We have derived a relationship between  $R_{BLR}$  and luminosity in the UV domain (1350 Å at rest frame), which exhibits a slope consistent with that of Kaspi et al. (2005), although slightly flatter and steeper than proposed in the optical and near-UV by Kaspi et al. (2000) and McLure & Jarvis (2002), respectively.

For those 10 blazars having multiwavelength spectral fits we have also applied an independent method of BLR size determination, based on the combination of the observed  $L_{BLR}$  and fitted external radiation density (“SED” method). We have not found a clear correlation between the BLR sizes obtained with the two methods, with the largest deviations observed in the sense of a deficit of the “SED” radii with respect to those obtained with the empirical  $R_{BLR} - \lambda L_{\lambda}$  relationship. We conclude that the SED method yields a BLR size inconsistent with that derived from the continuum luminosity.

Our estimated BH masses have an average of  $(2.8 \pm 2.0) \times 10^8 M_{\odot}$  (the quoted uncertainty is the standard deviation) and are comparable with those of lower redshift blazars, estimated with different methods (Barth, Ho, Sargent 2003; Falomo, Carangelo, & Treves 2003).

The distribution of our blazar BH masses computed with Eq. 5 is consistent with the distribution of the PG quasar masses computed with the same equation. These results suggest that the differences between radio powerful sources and radio-weak ones are not

due to the mass of the BHs residing at their centers. However, the validity of this conclusion at the intermediate/high redshifts must be corroborated by the analysis of wider samples of homogeneous datasets. Moreover, further intensive spectroscopic monitoring of the brightest blazars at optical and UV wavelengths is required, in order to construct well sampled continuum and emission line light curves for the application of the reverberation mapping technique.

#### ACKNOWLEDGMENTS

We thank R. Bohlin for assistance with HST data analysis, G. Ghisellini for helpful discussion, and the referee, A. Koratkar, for a constructive report. We acknowledge the use of the SIMBAD and NED databases, publicly available online. This work was partially supported by the Italian Space Agency under the contract I/R/056/02.

#### REFERENCES

- Ballo, L., et al. 2002, *ApJ*, 567, 50
- Barth, A.J., Ho, L.C., & Sargent, W.L.W. 2003, *ApJ*, 583, 134
- Bechtold, J., Dobrzycki, A., Wilden, B., Morita, M., Scott, J., Dobrzycka, D., Tran, K.-V., & Aldcroft, T. 2002, *ApJS*, 140, 143
- Bloom, S.D., et al. 1997, *ApJ*, 490, L145
- Bregman, J.N., et al. 1986, *ApJ*, 301, 708
- Cardelli, J. A., Clayton, G. C. & Mathis, J. S. 1989, *ApJ*, 345, 245
- Celotti, A., Padovani, P., & Ghisellini, G. 1997, *MNRAS*, 286, 415
- Corbett, E. A., Robinson, A., Axon, D. J., Hough, J. H., Jeffries, R. D., Thurston, M. R., & Young, S. 1996, *MNRAS*, 281, 737
- Courvoisier, T. J.-L. 1998, *A&AR*, 9, 1
- D'Elia, V., Padovani, P., & Landt, H. 2003, *MNRAS*, 339, 1081
- Dermer, C. D. & Schlickeiser, R. 1993, *ApJ*, 416, 458
- Evans, I. N., & Koratkar, A. P. 2004, *ApJS*, 150, 73
- Falomo, R., Kotilainen, J., Carangelo, N., & Treves, A. 2003, *ApJ*, 595, 624
- Fossati, G., Maraschi, L., Celotti, A., Comastri, A., Ghisellini, G. 1998, *MNRAS*, 299, 433
- Francis, P. J., Hewett, P. C., Foltz, C. B., Chaffee, F. H., Weymann, R. J., & Morris, S. L. 1991, *ApJ*, 373, 465
- Ghisellini, G., Padovani, P., Celotti, A., & Maraschi, L. 1993, *ApJ*, 407, 65
- Ghisellini, G., Celotti, A., Fossati, G., Maraschi, L., & Comastri, A. 1998, *MNRAS*, 301, 451
- Ghisellini, G., & Madau, P. 1996, *MNRAS*, 280, 67
- Grandi, P., & Palumbo, G.G.C. 2004, *Science*, 306, 998
- Haardt, F., et al. 1998, *A&A*, 340, 35
- Hartman, R. C., et al. 1999, *ApJS*, 123, 79
- Hartman, R. C., et al. 2001, *ApJ*, 553, 683
- Impey, C.D. & Tapia, S. 1988, *ApJ*, 333, 666
- Impey, C.D. & Tapia, S. 1990, *ApJ*, 354, 124
- Impey, C.D., Lawrence, C.R., & Tapia, S. 1991, *ApJ*, 375, 46
- Kaspi, S., Smith, P.S., Netzer, H., Maoz, D., Jannuzi, B.T., Giveon, U. 2000, *ApJ*, 533, 631
- Kaspi, S., Maoz, D., Netzer, H., Peterson, B.M., Vestergaard, M., & Jannuzi, B.T., 2005, *ApJ*, in press (astro-ph/0504484)
- Koratkar, A., Pian, E., Urry, C. M., & Pesce, J. E. 1998, *ApJ*, 492, 173
- Korista, K.T., et al. 1995, *ApJS*, 97, 285
- Kuraszkiewicz, J. K., Green, P. J., Forster, K., Aldcroft, T. L., Evans, I. N., & Koratkar, A. 2002, *ApJS*, 143, 257
- Kuraszkiewicz, J. K., Green, P. J., Crenshaw, D. M., Dunn, J., Forster, K., Vestergaard, M., & Aldcroft, T. L. 2004, *ApJS*, 150, 165
- Liang, E.W., & Liu, H.T. 2003, *MNRAS*, 340, 632
- Maraschi, L., & Tavecchio, F. 2003, *ApJ*, 593, 667
- Mattox, J. R., Wagner, S. J., Malkan, M., McGlynn, T. A., Schachter, J. F., Grove, J. E., Johnson, W. N., & Kurfess, J. D. 1997, *ApJ*, 476, 692
- McLure, R. J., & Dunlop, J. S. 2001, *MNRAS*, 327, 199
- McLure, R. J., & Dunlop, J. S. 2002, *MNRAS*, 331, 795
- McLure, R. J., & Jarvis, M. J. 2002, *MNRAS*, 337, 109
- McLure, R. J., & Dunlop, J. S. 2004, *MNRAS*, 352, 1390
- Netzer, H., et al. 1994, *ApJ*, 430, 191
- Onken, C.A., & Peterson, B.M. 2002, *ApJ*, 572, 746
- Padovani, P., & Urry, C. M. 1992, *ApJ*, 387, 449
- Padovani, P., & Giommi, P. 1995, *ApJ*, 444, 567
- Padovani, P., Perlman, E. S., Landt, H., Giommi, P., & Perri, M. 2003, *ApJ*, 588, 128
- Paltani, S., & Türler, M. 2005, *A&A*, 435, 811
- Perlman, E.S., et al. 1996, *ApJS*, 104, 251
- Peterson, B. M., & Wandel, A. 2000, *ApJ*, 540, L13
- Peterson, B.M., Ferrarese, L., Gilbert, K.M., et al. 2004, *ApJ*, 613, 682
- Pian, E., Urry, C.M., Maraschi, L., et al. 1999, *ApJ*, 521, 112
- Pian, E., Falomo, R., Hartman, R. C., et al. 2002, *A&A*, 392, 407
- Scarpa, R., Falomo, R., & Pian, E. 1995, *A&A*, 303, 730
- Scarpa, R., & Falomo, R. 1997, *A&A*, 325, 109
- Schlegel, D.J., Finkbeiner, D.P., & Davis, M. 1998, *ApJ*, 500, 525
- Sikora, M., Begelman, M. C., & Rees, M. J. 1994, *ApJ*, 421, 153
- Spergel, D. N., Verde, L., Peiris, H. V. et al. 2003, *ApJS*, 148, 175
- Stickel, M., Padovani, P., Urry, C. M., Fried, J. W., & Kühr, H. 1991, *ApJ*, 374, 431
- Stoeckle, J.T., Morris, S.L., Gioia, I.M., Maccacaro, T., Schild, R., Wolter, A., Fleming, T.A., & Henry, J.P. 1991, *ApJS*, 76, 813
- Telfer, R.C., Zheng, W., Kriss, G.A., & Davidsen, A.F. 2002, *ApJ*, 565, 773
- Ulrich, M. H., Boksenberg, A., Bromage, G., et al. 1980, *MNRAS*, 192, 561
- Vermeulen, R. C., Ogle, P. M., Tran, H. D., Browne, I. W. A., Cohen, M. H., Readhead, A. C. S., Taylor, G. B., & Goodrich, R. W. 1996, 1995, *ApJ*, 452, L5
- Vestergaard, M. 2002, *ApJ*, 571, 733
- Wall, J.V., & Peacock, J.A. 1985, *MNRAS*, 216, 173
- Wandel, A. 1999, *ApJ*, 519, L39
- Wandel, A., Peterson, B.M., & Malkan, M.A. 1999, *ApJ*, 526, 579
- Wang, J.-M., Luo, B., & Ho, L.C. 2004, *ApJ*, 615, L9
- Wehrle, A. E., Pian, E., Urry, C. M., et al. 1998, *ApJ*, 497, 178
- Wills, B.J., Wills, D., Breger, M., Antonucci, R.R.J., & Barvainis, R. 1992, *ApJ*, 398, 454
- Wills, B.J., Thompson, K.L., Han, M., Netzer, H., Wills, D., Baldwin, J.A., Ferland, G.J., Browne, I.W.A., & Brotherton, M.S. 1995, *ApJ*, 447, 139
- Woo, J.-H., Urry, C. M. 2002, *ApJ*, 579, 530
- Zheng, W., Kriss, G.A., Telfer, R.C., Grimes, J.P., & Davidsen, A.F. 1997, *ApJ*, 475, 469

**Table 2: Emission Lines Measurements**

Object	$z$	$\text{Ly}\beta^a$		$\text{Ly}\alpha^a$		Si IV		C IV		C III		Mg II	
		EW <sup>b</sup>	FWHM <sup>b</sup>	EW	FWHM	EW	FWHM	EW	FWHM	EW	FWHM	EW	FWHM
BL0403-1316	0.571	–	–	135 ± 4	14	9.8 ± 0.7	22	128 ± 4	17	26 ± 1	18	33 ± 3	30
BL0420-0127	0.915	–	–	105 ± 6	11	7.2 ± 0.8	19	56 ± 2	17	–	–	–	–
BL0537-4406	0.896	–	–	20 ± 2	12	1.7 ± 0.4	13	11.4 ± 0.7	11	–	–	–	–
BL0637-7513	0.656	11 ± 2	15	89 ± 2	11	4.5 ± 1	19	43 ± 2	11	12 ± 1	13	–	–
BL0954+5537	0.901	–	–	40 ± 1	11 <sup>c</sup>	–	–	25 ± 1	12 <sup>c</sup>	–	–	–	–
BL1144-3755	1.048	–	–	4.1 ± 0.6	14	–	–	4.6 ± 0.8	14	–	–	–	–
BL1156+2931	0.729	–	–	12.0 ± 0.8	18	1.1 ± 0.3	20	8.5 ± 0.5	26	–	–	–	–
BL1226+0219 <sup>d</sup>	0.158	2.6 ± 0.5	15	52 ± 2	12	–	–	26.8 ± 0.9	18	8.8 ± 0.3	19	6.6 ± 0.5	24
BL1226+0219 <sup>e</sup>	0.158	–	–	43 ± 3	14	–	–	31 ± 2	19	9.1 ± 0.6	24	8.5 ± 0.6	25
BL1229-0207	1.045	12 ± 1	13	94 ± 4	13	5.7 ± 0.5	25	42 ± 2	19	–	–	–	–
BL1253-0531	0.538	–	–	22 ± 1	13	–	–	20 ± 1	20 <sup>c</sup>	3.9 ± 0.5	15	6.4 ± 0.5	24
BL1611+3420	1.401	18 ± 2	26	58 ± 2	14	6.3 ± 0.9	27	48 ± 2	24	7 ± 1	34	–	–
BL1641+3954 <sup>f</sup>	0.595	–	–	67 ± 3	15	6 ± 1	20	71 ± 3	24	14.8 ± 0.9	21	22 ± 1	39
BL1641+3954 <sup>g</sup>	0.595	–	–	149 ± 36	14	16 ± 5	28	150 ± 16	22	45 ± 8	27	91 ± 19	25
BL2223-0512	1.404	23 ± 2	15	120 ± 3	10	–	–	58 ± 5	19	14 ± 3	40	–	–
BL2230+1128	1.037	–	–	77 ± 2	13	2.9 ± 0.4	19	29 ± 1	15	10.8 ± 0.6	21	–	–
BL2243-1222	0.63	16 ± 2	13	102 ± 2	10	8.5 ± 0.7	19	55 ± 1	12	13.3 ± 0.6	13	–	–
BL2251+1552 <sup>h</sup>	0.859	15 ± 1	12	89 ± 2	11	3.2 ± 0.5	25	31.8 ± 0.8	16	13.4 ± 0.7	24	–	–
BL2251+1552 <sup>i</sup>	0.859	8.3 ± 0.7	11	50 ± 1	14	–	–	16.8 ± 0.4	14	–	–	–	–
BL2251+1552 <sup>j</sup>	0.859	–	–	74 ± 7	11	–	–	36 ± 3	18	12 ± 2	18	–	–

<sup>a</sup> The  $\text{Ly}\alpha$  and  $\text{Ly}\beta$  line EW measurements may have a residual contamination by the N V  $\lambda 1240$  and O VI  $\lambda 1034$  lines, respectively. This possible contamination does not exceed  $\sim 10\%$ . We have deblended the contamination in the FWHM measurements.

<sup>b</sup> At rest frame, in Å. Uncertainties on the FWHM values are about 15%.

<sup>c</sup> This line has an asymmetric profile, with a more prominent red wing.

<sup>d</sup> 16.8 Jan 1991.

<sup>e</sup> 9.4 Jul 1991.

<sup>f</sup> 7.9 Jun 1992.

<sup>g</sup> 20.4 Aug 1995.

<sup>h</sup> 11.9 Sep 1991.

<sup>i</sup> 15.3 Nov 1991.

<sup>j</sup> 19.4 Aug 1995.